Femoral Nailing Through the Trochanter: The Reamer Pathway Indicates a Helical Nail Shape

Larry W. Ehmke, MS,* Britton M. I. Polzin, MD,† Stephen M. Madey, MD,* and Michael Bottlang, PhD*

Objectives: This biomechanical study captured the reamer pathway in human femurs reamed through a greater trochanteric entry portal. The spatial pathway of the reamed intramedullary canal was analyzed to determine how closely a helix can match the dimensions of this canal.

Methods: Twenty-one human cadaveric femurs were reamed through a trochanteric entry portal 12 mm lateral to the superior trochanteric border. The pathway of the reamer canal was measured with a 3-dimensional motion tracking sensor. The magnitude and direction of curvature along the reamed canal was calculated and an average canal pathway was determined. Finally, a best-fit helix was derived by comparing the average canal pathway with 90 different computer-generated helix pathways.

Results: The reamed canal exhibited a medially directed curvature of 1.97 ± 0.30 m^{-1} magnitude proximally and an anteriorly directed curvature of 1.21 ± 0.27 m^{-1} magnitude in the midsection. This multiplanar curvature could best be approximated by a helix with 1000 mm radius and 0.6 degree/mm pitch. This helix coincided within ± 1 mm with the reamed canal over 59% of the canal length. It deviated 4 mm medial and 7 mm posterior at the entry portal and 7 mm medial and 3 mm posterior at the distal end of the reamed canal.

Conclusion: These results provide a scientific rationale for the design of helically shaped intramedullary nails. Helical nails introduced through a trochanteric entry site may offer reduced bone stresses, ease insertion, and facilitate removal. This in turn may reduce the likelihood of iatrogenic intraoperative fracture.

Key Words: femur, nailing, trochanteric nail, geometry, helix

INTRODUCTION

In 1940 Küntscher introduced intramedullary nailing and advocated nail insertion through the greater trochanter.[1] His intramedullary nail was straight and had a slotted, hollow cross-section. This rather flexible design enabled nails to elastically conform to both the antecurvature in the femoral diaphysis and the lateral bend in the proximal femur toward the trochanteric entry portal. Along with interlocking technology came the need for stronger nails, which had a closed cross-section for better load support.[2] As nail designs increased in strength, trochanteric insertion of straight nails caused complications as a result of the geometric mismatch between the nail and its pathway in the femoral canal. Complications included iatrogenic fractures, varus malalignment, and comminution at the fracture site.[2–4] To circumvent these complications, nails have been conformed to account for the curvature of the femoral canal. In nails with a multiplanar curvature, such as the Zickel nail with a trochanteric entry site, refracture occurred during nail removal because the implant was not extracted along a single path.[5–7] Consequently, only a single curvature has been adopted in many contemporary nail designs, accounting for the femoral antecurvature.[8] These contemporary nails constitute the standard of care and have largely overcome complications encountered with earlier nail designs, such as iatrogenic fractures and malalignment.[9,10] Based on this single-plane curvature design, nails are recommended for insertion through the piriformis fossa, located in line with the pathway of the femoral intramedullary canal.[8,11] However, antegrade femoral nailing through the piriformis fossa is associated with considerable iatrogenic soft-tissue injury,[12] prolonged reduction of abductor strength,[13,14] and persistent pain at the insertion site in up to 40% of patients.[15,16] The most severe complication in children and adolescents is avascular necrosis of the femoral head, which occurs at an incidence rate of 2–3%.[17] Furthermore, access to the piriformis fossa for accurate nail insertion is challenging, especially in patients who are morbidly obese.[18,19]

Nail insertion through the greater trochanter offers a number of advantages over the piriformis fossa because the lateral entry portal causes a lower risk of damage to either the blood supply of the femoral head or to the gluteal nerve.[19–21] It is technically easier and better accessible than nail insertion through the piriformis fossa, allowing for decreased operative and fluoroscopy time.[19,22] Furthermore, because the outer surface of the trochanter is relatively flat, it is less likely for an awl to slip, as is often the case at the piriformis fossa.[12] However, trochanteric insertion of a closed-section nail necessitates an implant that accommodates both the medially convex curvature in the proximal femur and the antecurvature of the femoral diaphysis to avoid malreduction,[4] increased localized cortex stress, femoral bursting, and iatrogenic fracture during nail insertion.[3,9,23] Despite these severe complications caused by a geometric mismatch between the

nail and the femoral geometry, the pathway of the reamed canal for trochanteric nailing has not been fully described to date. Furthermore, several studies have noted a mismatch between contemporary intramedullary nails and the ante-curvature of the femur and have called for a reappraisal of these implant designs.[8,24] Most recently, trochanteric nails that require gradual rotation during progressive insertion to accommodate their dual curvature have been reintro-duced.[20,22,25] Fernandez Dell'Oca proposed a trochanteric nail with a helical shape, which has a continuous spiral curvature.[25] Theoretically, such a helical nail would precisely follow its own path during insertion and removal, thereby minimizing the risk for iatrogenic fractures. However, no complete description on the pathway of the reamed canal for insertion of a trochanteric nail exists to provide a scientific basis for intramedullary nail design. As such, it remains unclear how closely the path of a trochanteric nail can be approximated by a helix.

This study evaluated the feasibility of a helix-shaped femoral nail that would facilitate ease of nail insertion through the trochanter and save implant removal along a helical pathway. The first objective of this study was to measure the pathway of a reamed canal for insertion of a trochanteric nail. The second objective was to determine how accurately a helix-shaped nail can match this reamed canal.

MATERIALS AND METHODS

Specimens and Reaming

Twenty-one fresh-frozen, right human femora were harvested from 10 female and 11 male white donors with an average age of 70 ± 12 years, range 41 to 86 years, and an average height of 174 ± 8 cm. The length of each femur was measured as the distance between the most proximal aspect of the femoral head and the most distal facet of the medial condyle using a digitizing stylus of an electromagnetic track-ing system (PCBird, Ascension Technology, Burlington, VT). Specimens were reamed *antegrade* through a trochanteric entry site according to standard procedures using a flexible reaming system (SynReam, Synthes USA, West Chester, PA). The entry site was centered on the greater trochanter in the sagittal plane and 12 mm lateral to the superior trochanteric border to minimize soft-tissue injury to the piriformis tendon

while optimizing accessibility (Figs. 1A, B).[12] A 3-mm guide pin was advanced into the proximal femur under C-arm fluoroscope visualization (Series 9600, OEC Medical Systems Inc, Salt Lake City, UT) in the anteroposterior and lateral view. A 13-mm cannulated straight reamer was placed over the guide pin to open the proximal cortex. Subsequently, a blunt-tip guide wire was advanced through the center of the femoral canal up to the epiphyseal scar (Fig. 1C). Specimens were progressively reamed with irrigation in 0.5-mm increments up to the distal metaphysis. Reaming was started with a 9-mm reamer bit and increased to an interference fit in the isthmus region, evident by the onset of audible rattle as the reamer bit advanced through the isthmus.

Reamed Canal Digitization

The spatial pathway of the reamed canal was measured with the electromagnetic motion tracking system, which captured the x, y, and z position of a miniature sensor with an accuracy of 1.8 mm over the measurement range. For suppres-sion of measurement artifacts caused by nearby ferromagnetic objects, femurs were rigidly mounted on a nonmetallic mea-surement table.[26] A femoral coordinate system was defined with an X-Y plane parallel to the table surface that contacted the femur at the posterior tip of the lesser trochanter and at the posterior aspects of the femoral condyles. The origin of the coordinate system coincided with the trochanteric entry site, and the x-axis intersected the intercondylar notch (Fig. 2A). The pathway through the center of the reamed femoral canal was captured by retracting the motion-tracking sensor along the reamed pathway. For this purpose, the 8 × 8 × 18-mm sensor was mounted on the tip of a flexible shaft for insertion into the reamed canal (Fig. 2B). The sensor was embedded in a cylinder of 13–19 mm, depending on the diameter of the reamed canal, to precisely trace the canal midline. After manual insertion, the sensor was pulled back through the canal with a retractor cable driven by an electric motor at a constant speed, while acquiring more than 500 equally spaced 3-dimensional data points of the reamed canal pathway. The motor was mounted on a separate table at a distance sufficient to preclude any detectable electromagnetic interference. Each canal was digitized 3 times to demonstrate repeatability. In addition, the periphery of the femur in the coronal and sagittal
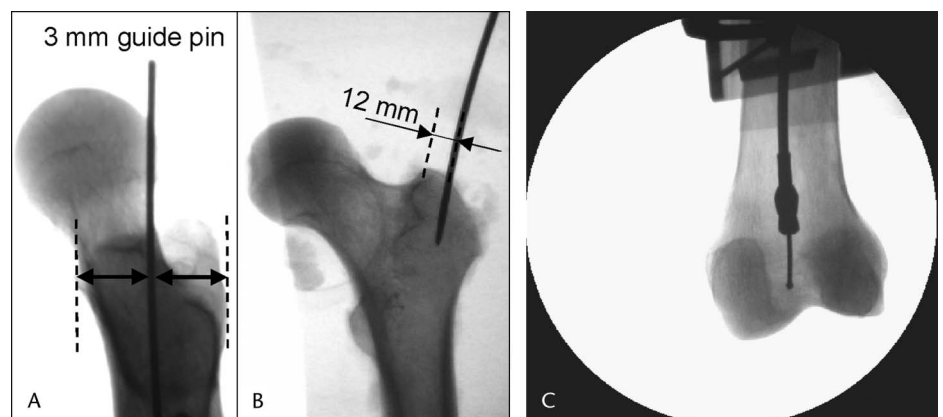

FIGURE 1. Antegrade reaming through a trochanteric entry portal, centered on the greater trochanter in the lateral view (A) and 12 mm laterally from the superior border (B). A flexible reamer was advanced to the epiphyseal scar (C).
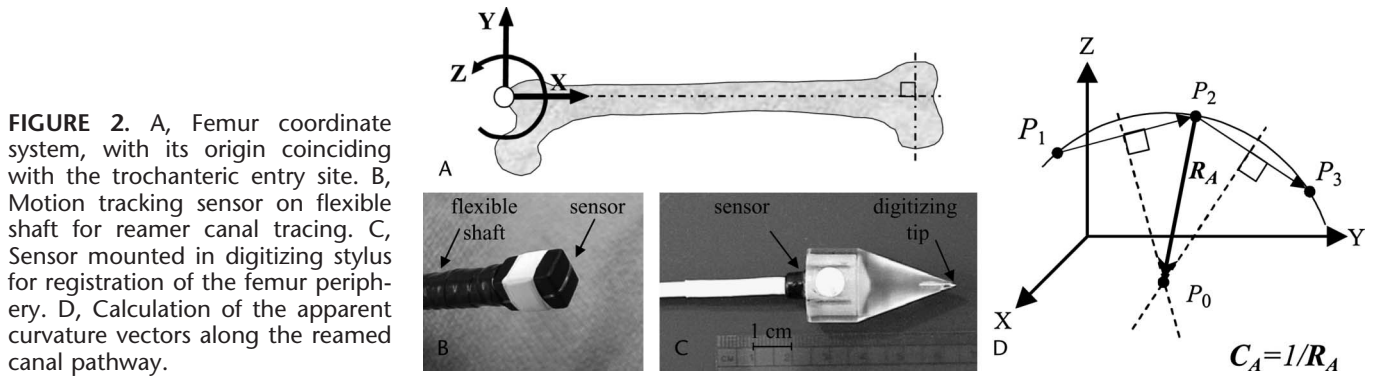
FIGURE 2. A, Femur coordinate system, with its origin coinciding with the trochanteric entry site. B, Motion tracking sensor on flexible shaft for reamer canal tracing. C, Sensor mounted in digitizing stylus for registration of the femur periphery. D, Calculation of the apparent curvature vectors along the reamed canal pathway.

plane was manually registered with the digitizing stylus to depict the femoral canal pathway in association with the anatomic profile of the femur (Fig. 2C).

Apparent Curvature of the Reamed Canal

Three noncollinear points—P_1, P_2, and P_3—on a curve segment define a unique circle in space with a radius vector $\overrightarrow{R_A}$ (Figure 2D). $\overrightarrow{R_A} = \overrightarrow{P_2 P_0}$ can be found by determining the intersect P_O of 2 lines, which bisect vectors $\overrightarrow{P_1 P_2}$ and $\overrightarrow{P_2 P_3}$ and which lie in the plane defined by P_1, P_2, and P_3. Assuming that small segments along the reamed canal curvature approximate regular arcs, the canal curvature can be completely characterized by a sequence of apparent radius vectors $\overrightarrow{R_A}$. The magnitude of $\overrightarrow{R_A}$ depicts the apparent curvature, and the direction of $\overrightarrow{R_A}$ defines the orientation of the apparent curvature.

A software algorithm for apparent curvature calculation was programmed in Matlab (The MathWorks, Natick, MA) and validated on a known curvature profile. For this purpose, a 20-mm deep and 20-mm wide arc segment of 500-mm radius was machined into the surface of a Plexiglas plate with an accuracy of 0.05 mm using a computer-numeric–controlled milling machine. To assess the accuracy and reproducibility of curvature computation, point triplets spanning 50-mm long arc segments were digitized 5 times with the motion tracking stylus for computation of 5 radius vectors $\overrightarrow{R_A}$. As a result of the difficulty of fabricating a curved tube of constant inner radius, this accuracy validation was performed by stylus digitization of a precision-machined curvature profile rather than by pulling a motion sensor through a curved tube.

After accuracy validation of the software algorithm, the apparent radius of the reamed canal was calculated in each specimen. Signal noise in canal tracings was reduced with a smoothing and spline fitting procedure. The spatial curvature profile was calculated along the reamed canal from point triplets with 20-mm spacing between points. Apparent radius vectors were extracted in 5% increments from 5% to 95% of the reamed canal, representing the medullary canal without extending into the distal metaphysis. For each 5% incremental location, results were presented in terms of the curvature magnitude $C_A = 1/R_A$ and in terms of the curvature orientation λ_A in the transverse plane. Curvature orientation values λ_A of 0

degrees, 90 degrees, 180 degrees, and 270 degrees represented convex curvatures in posterior, medial, anterior, and lateral directions, respectively. According to this definition, the antecurvature of the femoral diaphysis represented a convex curvature in anterior direction (λ_A = 180 degrees), with corresponding curvature vectors converging posteriorly.

Best-Fit Helix Calculation

To determine how closely the reamed canal for insertion of a trochanteric nail can be approximated by the best-fit helix formulation, the average pathway of the reamed canal was compared to the pathway of ideal helices. First, the average shape of the reamed canal was generated by normalizing the canal pathways of all 21 specimens to a representative canal length of 400 mm and by averaging pathway coordinates along the canal pathway. Subsequently, 90 helices $H_{(P,R)}$ were formulated as a function of the helix pitch H_P and the helix radius of curvature H_R, using Matlab software. H_P was varied from 90 degrees/400 mm to 360 degrees/400 mm in 30 degrees/400 mm intervals. H_R was varied from 800 to 1500 mm, in 100-mm increments, spanning the reported range of antecurvature of the femoral shaft.[8] For comparison to the reamed canal, each helix was aligned with the average pathway of the reamed canal in a manner that their trajectories coincided at 50% canal length, corresponding to the isthmus region. For each helix, the sagittal plane deviation Ψ_{sag} and the coronal plane deviation Ψ_{cor} between the helix and the average reamed canal pathway was computed at 10-mm increments along the pathway. The total deviation $\Psi_{total} = \Sigma(\Psi_{cor} + \Psi_{sag})$ was calculated as the sum of all coronal and sagittal plane deviations. The best-fit helix was extracted by determining the helix formulation with the smallest Ψ_{total} value. All outcome parameters were reported as the mean value $\pm$ 1 standard deviation.

RESULTS

On average, femurs were 460 $\pm$ 25 mm long, and the length of the reamed canals was 399 $\pm$ 26 mm. Thirteen specimens were reamed to 13 mm diameter, 7 specimens were reamed to 15 mm diameter, and 1 specimen was reamed to 19 mm diameter. Three repeat tracings of the reamed canal pathway, shown for 1 representative specimen in Figure 3,
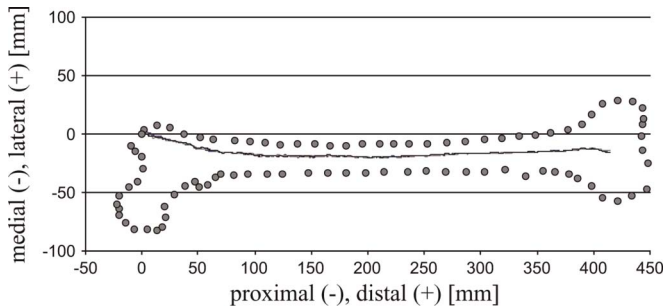
FIGURE 3. Coronal plane projections of 3 repeat tracings of the reamed canal pathway in 1 representative specimen.

deviated less than ±1.5 mm at the entry portal and were nearly indistinguishable in the remainder of the canal pathway. Calculating the apparent curvature from point triplets digitized on the machined arc segment of 500-mm radius yielded a radius magnitude of 511 ± 3 mm and a radius orientation that deviated 2.9 degrees ± 1.6 degrees from the plane of the arc segment.

The curvature magnitude C_A along the reamed canal exhibited 2 distinct regions of elevated curvature (Fig. 4A). The highest curvature of 1.97 m^{-1} was located at 20% of canal length from the trochanteric entry site. The second region of elevated curvature was located at 55% with $C_{55\%} = 1.21 \pm 0.27$ m^{-1}. The lowest curvature was observed in the most proximal section ($C_{5\%} = 0.49 \pm 0.15$ m^{-1}) and the most distal section ($C_{95\%} = 0.41 \pm 0.25$ m^{-1}) of the reamed canal.

The curvature orientation λ_A in the transverse plane ranged from $\lambda_{5\%} = 64$ degrees ± 9 degrees to $\lambda_{70} = 195$ degrees ± 25 degrees (Fig. 4B). It remained between 64 and 88 degrees over the proximal 30% of the canal length, whereby 90 degrees denotes a convex curvature in medial direction, with corresponding radius vectors converging laterally. In the canal region from 30% to 50%, λ_A gradually increases to 184 degrees ± 15 degrees, with 180 degrees denoting a canal curvature toward anterior. This antecurvature continued for the distal half of the reamed canal, whereby λ_A exhibited elevated standard deviations for canal segments beyond 75% of canal length.

The apparent curvature profile along the pathway of the average reamed canal demonstrates the medial bend in the proximal canal region and the antecurvature in the canal midsection (Fig. 5A). These curvature vectors gradually rotate around the canal pathway as the medially directed bend in the proximal pathway transitions into the antecurvature of the canal midsection. In the transverse plane, this rotation advances from $\lambda_{20\%} = 69$ degrees to $\lambda_{55\%} = 189$ degrees over a 140-mm long segment of the average reamed canal (Fig. 5B). Comparing this pathway of the average reamed canal to 90 plausible helix configurations yielded a best-fit helix that minimized the total deviation between the reamed canal and a given helix in the coronal and sagittal planes (Fig. 6). This best-fit helix had a radius of 1000 mm and a pitch of 240 degrees/400 mm. Its pathway coincided within ±1 mm with the average reamed canal over 59% of the canal length, from 21% to 80% (Fig. 7). Proximally, the entry site of the best-fit
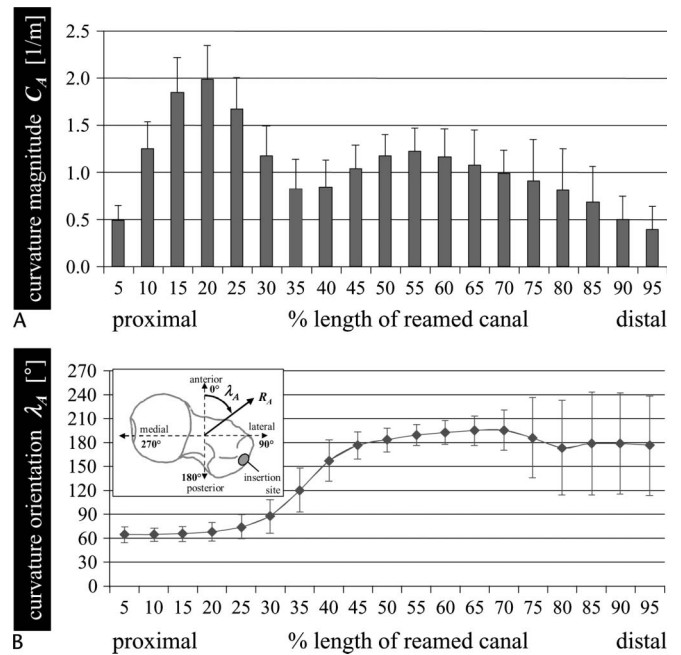

FIGURE 4. Apparent curvature profile of the reamed canal pathway: A, Profile of the curvature magnitude C_A. B, Profile of curvature orientation λ_A.

helix was 4 mm medial and 7 mm posterior from the entry site of the reamed canal. Distally, the helix deviated 7 mm medial and 3 mm posterior from the average reamed canal.

DISCUSSION

Results of this study expand on prior investigations of the femoral antecurvature by providing a comprehensive characterization of the femoral geometry pertinent to trochanteric nailing. This study provides new information that quantifies the 3-dimensional anatomy of the reamed intramedullary canal. These results are significant because they were obtained from the actual canal, not by inference from the cortical boundaries, and provide evidence supporting the redesign of intramedullary nails to approximate a helical shape.

Results of the present study describe the antecurvature orientation to be $\lambda_{55\%} = 189$ degrees ± 14 degrees. The reported radius of curvature in the middiaphyseal region ($R_{50\%} = 1/C_{50\%} = 884 \pm 187$ mm) is at the lower range of radii reported by Harper et al (689–1885 mm), Egol et al (530–3260 mm), and Zuber et al (600–2300 mm). Harper et al investigated the antecurvature of the intramedullary canal on lateral radiographs of 14 human femurs by digitizing 15 points along the femoral diaphysis.[8] Egol et al determined the femoral antecurvature of 948 paired femurs by using a 3-point circle function from commercially available software (AutoCAD).[24] Zuber et al determined from radiographs of 100 human femurs the antecurvature and the curvature *orientation* plane, which was 15 degrees anterolaterally, or at $\lambda = 195$ degrees according to the convention of the present study.[27] Furthermore, the radii of curvature of the present study were smaller than radii

FIGURE 5. A, Average reamed canal and apparent curvature profile, illustrating the medial bend in the proximal canal region, and the antecurvature in the canal midsection. B, Transverse plane projection of the average curvature vectors corresponding to the peak curvature in the proximal region ($\lambda_{20\%}$ = 69 degrees) and midsection ($\lambda_{55\%}$ = 189 degrees).
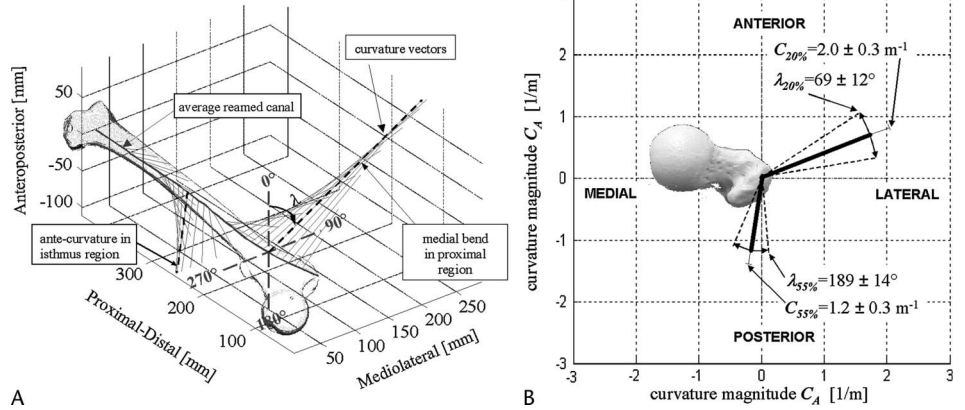
of contemporary intramedullary nails, which range from 1320 mm (3M, St. Paul, MN) to 4050 mm (Grosse-Kemp, Howmedica, Rutherford, NJ).[24,27]

Results of this study further defined a helix that closely follows the pathway of the reamed canal. This helix has a radius of 1000 mm and a pitch of 240 degrees/400 mm. The rational for a helical geometry of trochanteric nails was postulated by Fernandez Dell'Oca in 2002 to reduce localized cortex stress and femoral bursting during nail insertion and removal.[25] Fernandez Dell'Oca derived a helical nail shape by applying templates to planar radiographs of cadaveric femurs, but he did not report quantitative information on the helical nail shape. Subsequently, his nail was inserted in 17 patients. Fernandez Dell'Oca emphasized the potential benefit of helical nails for nail removal, whereby a helix can be retracted along its own pathway by gradual rotation, unlike nails with an irregular multiplanar curvature.

In the present study, the best-fit helix has an entry site located 8 mm lateral from the tip of the greater trochanter and 7 mm posterior to the trochanteric midline. This location at the posterolateral boundary of the piriformis tendon insertion closely approximates the favored entry portal reported for antegrade nailing, based on soft-tissue preservation and accessibility.[12] To the contrary, Ostrum et al found for contemporary trochanteric nails that the tip of the greater trochanter is close

to a "universal" starting point, whereas a lateral starting point leads to varus and gapping of a subtrochanteric fracture.[28] However, none of the trochanteric nail designs tested had a continuous helical shape. The distal tip of the best-fit helix deviates 7 mm medially from the reamed canal axis. This mild distal curvature of the helical nail will not impede placement of interlocking screws, but it may potentially obstruct a surgeon's ability to use the nail as a guideline to restore distal femur alignment.

This study has several limitations. It quantified the geometric deviation of an ideal helix pathway from the reamed canal, but it did not investigate the force required for insertion of a nail with an ideal helix shape. In addition to nail geometry, the insertion force and consequential strain in the femoral cortex also depends on bone quality and can be reduced by overreaming with a larger reamer. However, at the time of nail removal, heterotrophic ossification at the entry portal and fracture site can constrain the nail pathway to the actual nail dimension, in which case a helical nail can potentially reduce extraction forces as compared to nails with a nonhelical multiplanar curvature. The reported reamer canal pathway is specific for the entry portal chosen and the flexible reamer system used. The reamer type and shaft stiffness will likely affect the reamed canal curvature. In addition, the reported reamer canal pathways are representative of the elderly population because the specimens of this study were obtained from donors with an average age of 70 years. Furthermore, based on the limited sample size, specimens have not been stratified for gender, weight, or canal diameter. Despite this absence of stratification, a close match between the average reamed canal and the best-fit helix was found. As a logical next step, future studies should address helical nail shapes that account for patient gender, race, or morphometric parameters to further improve the fit between the reamed canal and a "best-fit" helical nail. Based on the relatively small curvature of the reamed canal, results of the apparent radius magnitude were expressed in terms of the curvature, which is the inverse of the radius magnitude. This improved the clarity of result graphs because the curvature of canal segments that approach a straight line converges to zero, whereas the corresponding radius increases exponentially. Furthermore, although the spatial orientation of apparent radius vectors is graphically
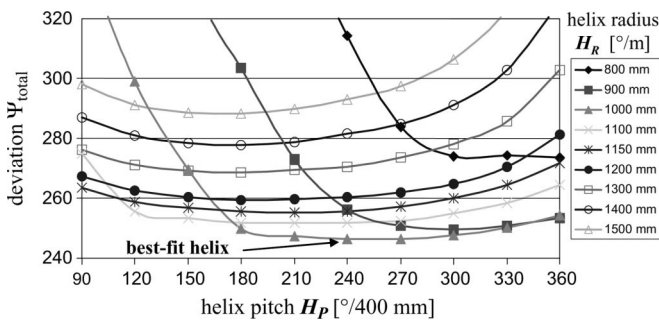

FIGURE 6. Accumulative deviation of the average reamed canal from an ideal helix, shown for 90 plausible helix configurations of specified pitch and radius. The best-fit helix (240 degrees/m pitch, 1000 mm radius) minimized Ψ_{total}.
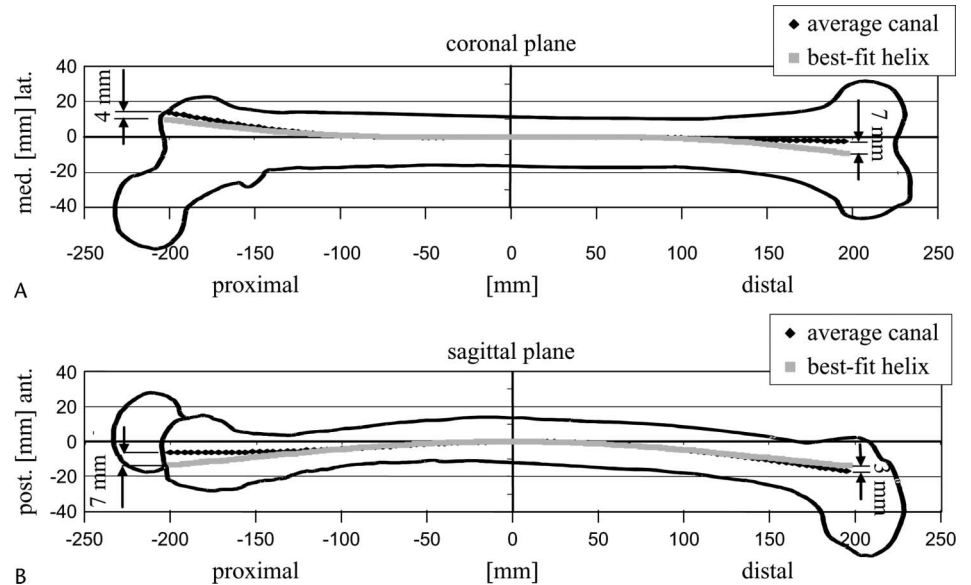
FIGURE 7. The best-fit helix, projected over the average reamed canal is shown in coronal projections (A) and in the sagittal plane (B).

displayed in Figure 5, radius orientation was subsequently reduced to transverse plane orientation λ to describe changes in curvature orientation along the reamed canal with a scalar outcome parameter.

In conclusion, the results of this study provided a quantitative description of the 3-dimensional characteristics of the reamed intramedullary canal that is created for insertion of a trochanteric nail. Despite wide variations in subjects studied, an ideal helical shape was found to fit the intramedullary canal over 59% of the mid shaft length. Consequently, a trochanteric intramedullary nail in the shape of such a helix can closely match the pathway of the reamer canal. This helical nail can facilitate ease of nail insertion through the greater trochanter and nail removal along a unique helical pathway. As such, results provide a biometric rationale for the geometry of intramedullary nails with a trochanteric entry portal. Results do not infer on the performance of trochanteric nails, and further studies are required to investigate insertion and removal forces of trochanteric nails with the proposed helical geometry.

REFERENCES

1. Bick EM. The intramedullary Nailing of Fractures by G. Kuntscher. Translation of article in Archiv fur Klinische Chirurgie, 200:443, 1940. *Clin Orthop Relat Res*. 1968;60:5–12.
2. Kempf I, Grosse A, Beck G. Closed locked intramedullary nailing. Its application to comminuted fractures of the femur. *J Bone Joint Surg Am*. 1985;67:709–720.
3. Johnson KD, Tencer AF, Sherman MC. Biomechanical factors affecting fracture stability and femoral bursting in closed intramedullary nailing of femoral shaft fractures, with illustrative case presentations. *J Orthop Trauma*. 1987;1:1–11.
4. Winquist RA, Hansen ST Jr, Clawson DK. Closed intramedullary nailing of femoral fractures. A report of five hundred and twenty cases. *J Bone Joint Surg Am*. 1984;66:529–539.
5. Ross PM, Kurtz N. Subcapital fracture subsequent to Zickel nail fixation: a case report. *Clin Orthop Relat Res*. 1980;131–133.
6. Yelton C, Low W. Iatrogenic subtrochanteric fracture: a complication of Zickel nails. *J Bone Joint Surg Am*. 1986;68:1237–1240.
7. Zickel RE. Intraoperative and postoperative subtrochanteric fracture of the femur associated with removal of the Zickel nail. *J Bone Joint Surg Am*. 1988;70:1428.
8. Harper MC, Carson WL. Curvature of the femur and the proximal entry point for an intramedullary rod. *Clin Orthop Relat Res*. 1987:155–161.
9. Simonian PT, Chapman JR, Selznick HS, et al. Iatrogenic fractures of the femoral neck during closed nailing of the femoral shaft. *J Bone Joint Surg Br*. 1994;76:293–296.
10. Yang KH, Han DY, Park HW, et al. Fracture of the ipsilateral neck of the femur in shaft nailing. The role of CT in diagnosis. *J Bone Joint Surg Br*. 1998;80:673–678.
11. Brumback RJ, Virkus WW. Intramedullary nailing of the femur: reamed versus nonreamed. *J Am Acad Orthop Surg*. 2000;8:83–90.
12. Dora C, Leunig M, Beck M, et al. Entry point soft tissue damage in antegrade femoral nailing: a cadaver study. *J Orthop Trauma*. 2001;15:488–493.
13. Bain GI, Zacest AC, Paterson DC, et al. Abduction strength following intramedullary nailing of the femur. *J Orthop Trauma*. 1997;11:93–97.
14. Danckwardt-Lilliestrom G, Sjogren S. Postoperative restoration of muscle strength after intramedullary nailing of fractures of the femoral shaft. *Acta Orthop Scand*. 1976;47:101–107.
15. Bednar DA, Ali P. Intramedullary nailing of femoral shaft fractures: reoperation and return to work. *Can J Surg*. 1993;36:464–466.
16. Dodenhoff RM, Dainton JN, Hutchins PM. Proximal thigh pain after femoral nailing. Causes and treatment. *J Bone Joint Surg Br*. 1997;79:738–741.
17. Orler R, Hersche O, Helfet DL, et al. [Avascular femur head necrosis as severe complication after femoral intramedullary nailing in children and adolescents]. *Unfallchirurg*. 1998;101:495–499.
18. McKee MD, Waddell JP. Intramedullary nailing of femoral fractures in morbidly obese patients. *J Trauma*. 1994;36:208–210.
19. Ostrum RF. A greater trochanteric insertion site for femoral intramedullary nailing in lipomatous patients. *Orthopedics*. 1996;19:337–340.
20. Moein CM, Verhofstad MH, Bleys RL, et al. Soft tissue injury related to choice of entry point in antegrade femoral nailing: piriform fossa or greater trochanter tip. *Injury*. 2005;36:1337–1342.

21. Townsend DR, Hoffinger S. Intramedullary nailing of femoral shaft fractures in children via the trochanter tip. *Clin Orthop Relat Res*. 2000: 113–118.
22. Ricci WM, Devinney S, Haidukewych G, et al. Trochanteric nail insertion for the treatment of femoral shaft fractures. *J Orthop Trauma*. 2005;19:511–517.
23. Miller SD, Burkart B, Damson E, et al. The effect of the entry hole for an intramedullary nail on the strength of the proximal femur. *J Bone Joint Surg Br*. 1993;75:202–206.
24. Egol KA, Chang EY, Cvitkovic J, et al. Mismatch of current intramedullary nails with the anterior bow of the femur. *J Orthop Trauma*. 2004;18:410–415.

25. Fernandez Dell'Oca AA. The principle of helical implants . Unusual ideas worth considering. *Injury*. 2002;33:19–27.
26. Bottlang M, Marsh JL, Brown TD. Factors influencing accuracy of screw displacement axis detection with a D.C.-based electromagnetic tracking system. *J Biomech Eng*. 1998;120:431–435.
27. Zuber K, Schneider E, Eulenberger J, et al. [Form and dimension of the bone marrow cavity of the human femur with reference to the fit of intramedullary implants]. *Unfallchirurg*. 1988;91:314–319.
28. Ostrum RF, Marcantonio A, Marburger R. A critical analysis of the eccentric starting point for trochanteric intramedullary femoral nailing. *J Orthop Trauma*. 2005;19:681–686.